Trials

RESEARCH

Open Access

A novel noninvasive assessment of portal pressure from computational biofluid mechanics in patients with portal hypertension

Lei Zheng[1†], Guangbo Wu[1†], Jiayun Lin[1†], Hongjie Li[1], Chihao Zhang[1], Zhifeng Zhao[1], Min Chen[1], Zhenghao Wu[1], Guqing Luo[1], Qiang Fan[1], Xiaoliang Qi[1], Haizhong Huo[1*], Longci Sun[2*] and Meng Luo[1*]

Abstract

Background and aims To introduce and assess a novel method for portal pressure measurement based on biofluid mechanics in portal hypertensive patients undergoing surgery.

Methods The research was a multi-center, retrospective study, conducted on patients who underwent surgery and measurement of free portal pressure (FPP). There were 118 patients included and 21 patients excluded due to the failure or poor results of Doppler ultrasound, and 97 patients were screened. We used patients' CT images, Doppler ultrasound results of the portal system, blood density and viscosity to reconstruct their portal system and simulate its internal blood flow. According to the patient's physical property, geometry, and boundary conditions, the Navier–Stokes equations were solved by FLUENT software, and virtual free portal pressure (vFPP) was calculated. Finally, the Bland–Altman Limits of Agreement, intraclass correlation coefficient (ICC), and the Lin's concordance correlation coefficient were performed to evaluate the numerical correlation between the vFPP and FPP.

Results All patients enrolled in this study underwent the surgery, and the FPP of patients was measured during the surgery, with a mean FPP of 22.8 ± 3.3 mmHg (range: 13–33 mmHg). Meanwhile, according to computational biofluid mechanics, all patients' vFPP was calculated. Then, we further explored whether there was a close relationship between vFPP and FPP in the whole population. For the analysis of Bland–Altman Limits of Agreement, the mean value of difference was − 0.1569 (95% CI: − 0.4305 to 0.1167); lower limit of agreement: − 2.8176 (95% CI: − 3.2868 to − 2.3484); upper limit of agreement: 2.5038 (95% CI: 2.0346 to 2.9730). The ICC was 0.9215 (95% CI: 0.8848 to 0.9468). Furthermore, the Lin's concordance correlation coefficient showed a numerical correlation between the vFPP and FPP, which was 0.9205 (95% CI: 0.8840 to 0.9459). All these results confirmed that our vFPP model could provide an accurate prediction of FPP in patients.

Conclusions The vFPP of patients calculated by computational biofluid mechanics was significantly correlated with the FPP of portal hypertensive patients, which would be a novel, non-invasive, and accurate method for the assessment of portal pressure in surgical patients.

Keywords Portal hypertension, Free portal pressure, Computational biofluid mechanics

[†]Lei Zheng, Guangbo Wu, and Jiayun Lin contributed equally to this article.

*Correspondence:
Haizhong Huo
luosh9hospital@sina.com
Longci Sun
renjisunlongci@163.com
Meng Luo
fireseah@163.com

Introduction

Portal hypertension (PHT), usually caused by sinusoidal, post-sinusoidal, and pre-sinusoidal causes, is a serious threat to patients with liver disease and a syndrome with high mortality [1]. The accurate detection of portal pressure is of great significance for the diagnosis, treatment, and prognosis of patients [2–5]. In present clinical and scientific research, there are various direct and indirect methods for measuring portal pressure. Hepatic vein pressure gradient (HVPG), an indirect reflection of portal pressure, is widely accepted as the gold standard representing portal pressure [6–8]. PHT is the main predictor for the bleeding of esophageal varices (EV), and other severe outcomes [9]. However, the measurement of free portal pressure (FPP) directly reflects portal pressure and has several advantages during the operation for surgeons [10, 11]. As a result, the measurement of FPP is a reliable indicator for the accurate assessment of portal pressure.

Although FPP is performed under invasive surgery, it is convenient for the patient to measure FPP during surgery. However, due to the inherent risks, including injury, bleeding, thrombosis, infection, and trauma, FPP is usually not used to assess and monitor the progress of chronic liver disease [12]. To date, noninvasive methods to detect portal venous pressure include the following: the detection of portal hemodynamics by contrast-enhanced ultrasound [10], rectal vein-portal vein radionuclide imaging approaches [13], magnetic resonance angiography [14], spiral computed tomography portography [15], liver transient elastography [16, 17], and detection under endoscopic ultrasonography (EUS) guidance [17, 18]. However, these non-invasive methods of detecting portal pressure are unreliable due to various interferences [2, 19]. Hence, a non-invasive, more accurate, and reliable quantitative evaluation of portal vein pressure has significant clinical value for patients with PHT.

Biofluid mechanics has been widely used in many fields. It studies the basic mechanics of biological flow and its relationship with pathological and physiological processes by using the basic principles of fluid mechanics [20, 21]. It has diverse applications in artificial vascular, bypass surgery, artificial heart valves, dialysis shunts, anastomosis techniques, and vascular stents [22–24]. James K. Min et al. first put forward fractional flow reserve, which was computed from coronary CTA to noninvasively diagnose coronary stenosis, showing a good diagnostic performance in a multi-center, retrospective clinical study that involved 252 patients across five countries [25]. This ingenuity prompts us to search for non-invasive techniques for evaluating portal pressure. Although Qi et al. applied similar methods to portal pressure assessment and showed good diagnostic performance in evaluating portal pressure, however, the researchers did not take into account the fluid parameters (such as viscosity and density), which might affect the result, thus further research is needed [26–28].

The application of the biofluid mechanics to the patients' portal system requires geometry, anatomy, blood flow rate, and reliable methods of velocity and volume measurement [29, 30]. The blood flow parameters of individuals can be evaluated in a portal vein system using imaging measurement methods (e.g., multi-slice spiral CT angiography (CTA) or color Doppler ultrasound). Furthermore, physical parameters, especially blood density and blood viscosity (BV) of portal vein blood at different shear rates, are equally important to determine the portal vein biofluid mechanics data [31]. In previous studies, our research group focused on the construction of a model based on biofluid mechanics, which can accurately and reliably detect free portal vein pressure and predict portal pressure in canines [32]. However, whether this model can be used to calculate human FPP, evaluating disease progress and therapeutic effect remains to be further studied and verified.

To sum up, in order to establish a novel and more reliable model for portal pressure measurement, the investigators conducted a multi-center retrospective study on Chinese patients with PHT. Virtual free portal pressure (vFPP) was calculated by biofluid mechanics methods and compared to FPP.

Materials and methods

Study population

This study was performed in patients who underwent periesophagogastric devascularization combined with splenectomy or Warren shunt because of severe esophageal varices or hypersplenism from January 2015 to June 2021 at the General Surgery Department of Shanghai Ninth People's Hospital and the Department of Gastrointestinal Surgery of Shanghai Renji Hospital.

Inclusion criteria

1. Patients aged 20–90 years old.
2. Patients diagnosed as PHT by clinical symptom, imaging examination (MRI, CT, ultrasound, and FibrosScan) or liver biopsy, treatment for FPP assessment, and surgery.

Exclusion criteria

1. Patients with unstable conditions or patients with unpredictable clinical processes.
2. Female patients who are pregnant or breastfeeding.
3. Patients suffering from clinically unstable heart diseases, such as congenital cardiac disorder, cardiac arrhythmia, and severe heart failure.
4. Patients suffering from clinically unstable pulmonary disease or acute respiratory distress syndrome.
5. Patients suffering from severe coagulopathy.
6. Patients suffering from a hepatic vein, portal vein, mesenteric vein occlusion, or thrombosis.
7. Patients suffering from ascites, hepatocarcinoma, or hepatic compensatory disorder.

Assessment

All enrolled patients were adequately evaluated for demographic parameters, etiology of PHT, liver function, and the severity of PHT. Patients underwent surgery within one month after evaluation and no treatments that may affect FPP values were taken during this period. A standard methodology was followed for the surgery and the measurement of FPP. Portal hypertension-related surgery and FPP measurement were performed following standard methods. Patients were examined for FPP immediately after abdominal incision. FPP was measured immediately after opening the abdominal cavity. During the operation, the patient took the supine position, and the axillary midline was taken as the baseline for measuring FPP. The gastrocolic ligament was cut off along the transverse colon. A silicone catheter with a diameter of 0.3 cm and a length of 20 cm was inserted into the main portal vein through the right branch of the middle colonic vein and superior mesenteric vein (approximately 15 cm in length). Then, we fixed the catheter and connected it to the pressure monitor (Edwards Lifesciences TruWave PX260, USA), and the FPP was obtained.

3D portal venous model

All patients underwent CT after being hospitalized on an empty stomach. The CT device used for the portal system was the Philips Brilliance CT Lightspeed-64 multi-slice spiral scanner. The following arguments were used: slice thickness, 0.625–2.5 mm; current, automatic; collimation, 1.24–1.25 mm; matrix size, 512×512; slice interval, 1.0–2.0 mm; rotation time, 0.5 s and voltage, 120 kVp. Patients were injected with non-ionic iodinated contrast agents (300–370 mg of iodine/mL, 600 mg of iodine/kg of body weight, 3–5 mL/s). Portal venous phase imaging was implemented 60–70 s after intravenous injection of contrast agent. Image data of CT was viewed by at least two CT specialists who were responsible for identifying the main branch of the portal vein, such as the right and left branches portal vein, the superior and inferior mesenteric vein, and the splenic vein.

The CT images were then imported into the IQQA liver system to construct a 3D portal venous model.

Laboratory parameters

Once these patients were hospitalized on an empty stomach, blood samples then were taken from the median cubital vein for a series of routine blood tests. The samples were immediately transferred into anticoagulant tubes for blood routine tests, liver function, routine coagulation examinations, and the blood viscosity test, while the remaining blood samples were used for density measurement. The routine blood tests were detected by Sysmex-5000 (Sysmex, Japan). The blood density was measured by weighing 1 mL of blood: a pipette was used to transfer 1 mL of blood to an electronic balance for weight measurement.

Doppler ultrasound data acquisition

All patients underwent Doppler ultrasound after being hospitalized on an empty stomach. The Doppler ultrasound was carried out to assess the maximum flow velocity and vascular inner diameter of the portal system, including the left and right branches and the main portal system, superior and inferior mesenteric vein, and splenic vein. Each measurement was made with deep breath holding, and intonation angles of $45^\circ - 55^\circ$ were used. The mean blood flow velocity approximately equals 0.7 times the maximum blood flow velocity. In order to guarantee the stability of the results, all measurements had three replicates, and the average values were finally calculated.

Computational biofluid mechanics

The geometric model was created from the CT Images using the IQQA software. Then, the model was imported into the Fluent software version 6.3 (ANSYS, Inc., USA) and its surface was divided into triangular surface meshes with the size of 0.2–1.0 mm, and the corresponding solid meshes were established. The laminar viscous model was used. The material type was set to fluid, and blood density and overall viscosity were used as the properties of the fluid. The pressure outlet boundary conditions module was used for the portal vein, with the following parameters: backflow reference frame: absolute; gauge pressure: 0; backflow direction specification method: normal to boundary; radial equilibrium pressure distribution: disabled; average pressure specification: disabled; target mass flow rate: disabled. The velocity inlet boundary conditions module was used for each inlet and outlet branch, with the following parameters: velocity specification

method: magnitude, normal to boundary; reference frame: absolute; supersonic/initial gauge pressure: 0. The velocity magnitude value was set to the blood flow velocity at the boundaries of each branch, which was calculated according to the inner diameter (obtained from the geometric model), the blood flow velocity (measured by Doppler ultrasound) and the principle of mass conservation. Considering the whole blood as a non-Newton fluid, the blood flow could be simulated using the following Navier–Stokes equations.

$$\frac{\partial \rho}{\partial t} + \nabla \bullet \left(\rho \overrightarrow{v}\right) = S_m \tag{1}$$

$$\frac{\partial \rho}{\partial t} + \frac{\partial}{\partial x}(\rho v_x) + \frac{\partial}{\partial r}(\rho v_r) + \frac{\rho v_r}{r} = S_m \tag{2}$$

$$\frac{\partial}{\partial t}(\rho E) + \nabla \bullet (\overrightarrow{v}(\rho E + p)) = \nabla \bullet \left(k_{eff} \nabla T - \sum_j h_j \overrightarrow{J}_j + (\overline{\overline{\tau}}_{eff} \bullet \overrightarrow{v})\right) + S_h \tag{3}$$

$$\frac{\partial}{\partial t}\left(\rho \overrightarrow{v}\right) + \nabla \bullet \left(\rho \overrightarrow{v} \overrightarrow{v}\right) = -\nabla p + \nabla \bullet \left(\overline{\overline{\tau}}\right) + \rho \overrightarrow{g} + \overrightarrow{F} \tag{4}$$

$$\overline{\overline{\tau}} = \mu \left[\left(\nabla \overrightarrow{v} + \nabla \overrightarrow{v}^T\right) - \frac{2}{3} \nabla \bullet \overrightarrow{v} I\right] \tag{5}$$

ρ: density; v: velocity; $E = h - \frac{p}{\rho} + \frac{v^2}{2}$; h: enthalpy value; p: pressure; $p\overrightarrow{g}$: gravity; $\overrightarrow{F}$: external body force; $\overline{\overline{\tau}}$: stress tensor; μ: viscosity; I: unit tensor.

Sample size calculation

Sample size was calculated by PASS Software V.19.0.1, (NCSS, LLC, USA). The "Bland–Altman Method for Assessing Agreement in Method Comparison Studies" procedure was used. The result showed that a sample of 112 subjects would achieve 80% power to detect agreement when the confidence level of the limits of agreement is 0.950, the confidence level of the CIs about the limits of agreement is 0.950, and the maximum allowable difference is 3.000. The mean and SD of the sample differences are anticipated to be 0.184 and 1.163, which were obtained from previous canine experiments. It is anticipated that 5% of the patients recruited are likely to be excluded due to various reasons and therefore the total sample size is 118 patients.

Statistical analysis

The test of continuous variable was normal distribution and represented by mean ± standard deviation (SD). The statistics were compared by Student's *t*-test. Repeated measures analysis of variance was utilized to compare FPP and vFPP in all patients, and Bland–Altman Limits of Agreement was used to analyze the numerical correlation between vFPP and FPP. The mean value of the difference between vFPP and FPP was regarded as bias. The standard deviation of the average difference of 1.96 was considered to be lower and upper limits of agreement. Lin's concordance correlation coefficient and intraclass correlation coefficient (ICC) were performed to analyze the numerical correlation between vFPP and FPP. In this study, the difference was statistically significant ($P < 0.05$). MedCalc statistical software and SPSS Statistics were used for statistical analysis (version 19.1.7, MedCalc Software bvba, Belgium; version 26.0, IBM, USA).

Results

General characteristics of the patients

In this study, there were 118 patients included and 21 patients excluded due to the failure or poor results of Doppler ultrasound, and 97 patients were screened (Fig. 1). A summary of patients' characteristics is given in Table 1. The mean age of these patients was 56 ± 12 years old (range: 28–89 years old), and the majority (73%) of these patients were males. The etiology of cirrhosis was classified as hepatitis B virus and hepatitis C virus (59, 61%), cholestatic cirrhosis (9, 9%), autoimmune liver disease (7, 7%), alcoholic cirrhosis (5, 5%), Budd-Chiari syndrome (1, 1%), and other reasons (including mixed etiology) (16, 17%). Hepatitis B virus and hepatitis C virus (61%) were the most common cause of liver cirrhosis in the Chinese population. Ascites occurred in 76% of patients. Furthermore, there were non-bleeders in 58% of patients, while the rest had bleeding from the varices in the past. For all patients who underwent the surgery, the mean FPP was 22.8 ± 3.3 mmHg (range: 13–33 mmHg).

Calculation for vFPP by computational biofluid mechanics

The obtained abdominal CTA images of PHT patients were imported into the IQQA liver system to construct the 3D portal venous model (Fig. 2A). In this model, the portal system, such as the right and left branches portal vein, superior and inferior mesenteric vein, and splenic vein, could be clearly seen. The body meshes of the model were created, as shown in Fig. 2B. Then, according to the model and Doppler ultrasound data, the boundary conditions were calculated. One situation is shown in Fig. 2C.

Afterwards, the pressure distribution of the portal system in vitro was calculated using the finite element

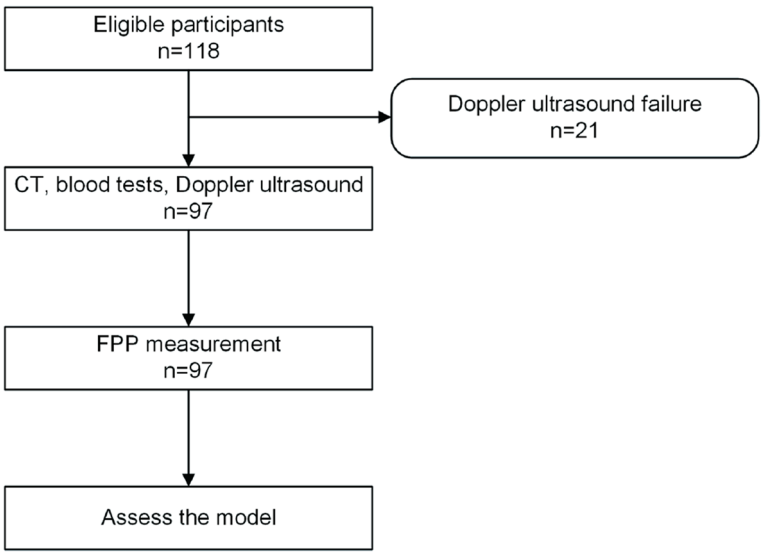

Fig. 1 Study procedure. FPP, free portal pressure

Table 1 Demographic profile of the study population

Parameters	Value ($n=97$)
Gender	
Males	71 (73%)
Females	26 (27%)
Age	56 ± 12 (28–89)
Etiology	
Viral (HBV/HCV)	59 (61%)
Cholestasis	9 (9%)
Autoimmune	7 (7%)
Alcohol	5 (5%)
Budd-Chiari syndrome	1 (1%)
Others (including mixed etiology)	16 (17%)
Ascites	
None	23 (24%)
Mild	46 (47%)
Moderate to tense	28 (29%)
Bleeding status	
Bleeder	41 (42%)
Non-bleeder	56 (58%)
FPP, mmHg	22.8 ± 3.3 (13–33)

analysis and computational biofluid dynamics method. In order to perfectly simulate the portal system in vivo, since blood was a Non-Newton fluid, blood density and the four levels of different shear stresses were measured, such as portal whole blood viscosities under the shear rates of BV 200 s^{-1}, BV 30 s^{-1}, BV 5 s^{-1}, and BV 1 s^{-1}. Finally, according to each patient's physical property, geometry, and boundary conditions, the Navier–Stokes equations were solved by FLUENT software, and vFPP was calculated, which was consistent with the PHT diagnosis of the patients. In addition, the velocity and pressure distribution of different sections in the portal system could be obtained simultaneously (Fig. 3).

The relationship between vFPP and FPP in the whole population

The numerical correlation between FPP and vFPP was analyzed mainly by using Bland and Altman's limits of agreement analysis. Bias, which is defined as the mean of the difference between FPP and vFPP, was − 0.1569 (95% CI: − 0.4305 to 0.1167); lower limit of agreement: − 2.8176 (95% CI: − 3.2868 to − 2.3484); upper limit of agreement: 2.5038 [95% CI: 2.0346 to 2.9730]. The numerical relationship between FPP and vFPP was also analyzed with the intraclass correlation coefficient and Lin's concordance correlation coefficient. The intraclass correlation was 0.9215 (95% CI: 0.8848 to 0.9468) and the Lin's concordance correlation coefficient was 0.9205 (95% CI: 0.8840 to 0.9459) (Fig. 4).

Discussion

The individualized treatment and prognosis of patients with chronic liver disease depend largely on the severity of PHT, so accurate detection of portal pressure is necessary. The method for the diagnosis of PHT in patients with chronic liver disease is the direct measurement of their portal pressure, such as the measurement of HVPG and FPP. The detection of HVPG is currently the gold standard for the diagnosis of intrahepatic PHT in patients [33, 34]. HVPG is below 5 mmHg in the healthy

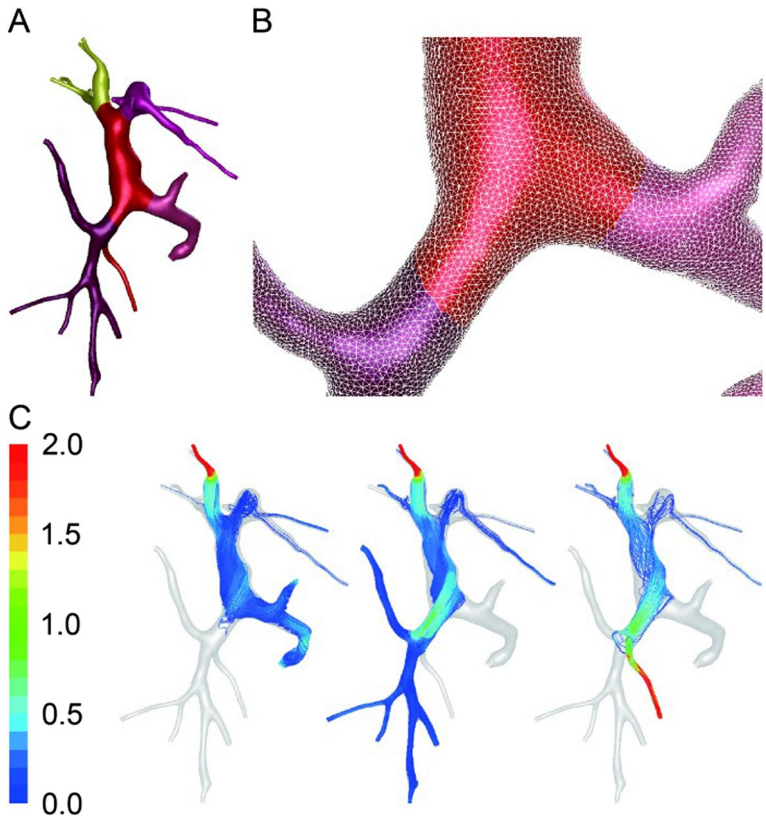

Fig. 2 An example of the simulation model of a portal venous system. **A** The geometry of the simulation model. **B** The body meshes of the simulation model. **C** The blood flow velocity (m/s) of the portal vein and its branches

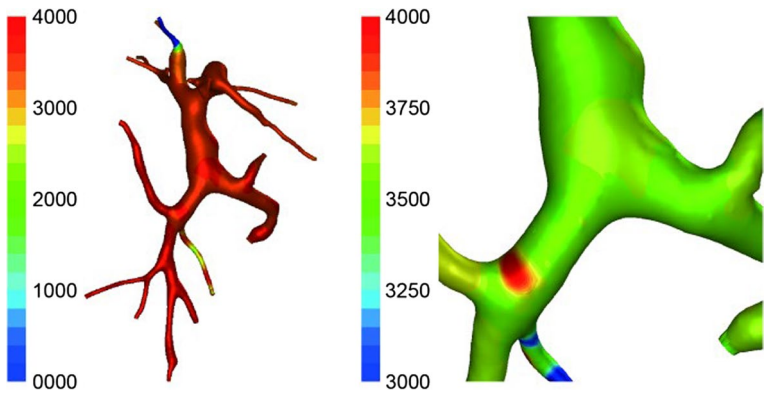

Fig. 3 An example of the blood pressure (Pa) of the portal vein and its branches

population. HVPG > 5 mmHg suggests the presence of PHT. When HVPG ≥ 10 mmHg, PHT-related complications such as ascites or variceal bleeding tend to occur, which is known as CSPH [35, 36]. Although HVPG has several advantages, it is rather difficult to perform HVPG measurements during operations and surgeons usually rely on the FPP for choosing appropriate surgical methods. For example, patients whose FPP is over 20 mmHg after splenectomy require a Warren shunt. So FPP is of great significance as a reliable indicator for the diagnosis of PHT caused by various chronic liver diseases.

Although HVPG and FPP measurements are relatively safe procedures, these are considered invasive methods, which have many contraindications as we described before. Thus, the development of novel non-invasive methods of PHT is encouraged [37]. Various methods

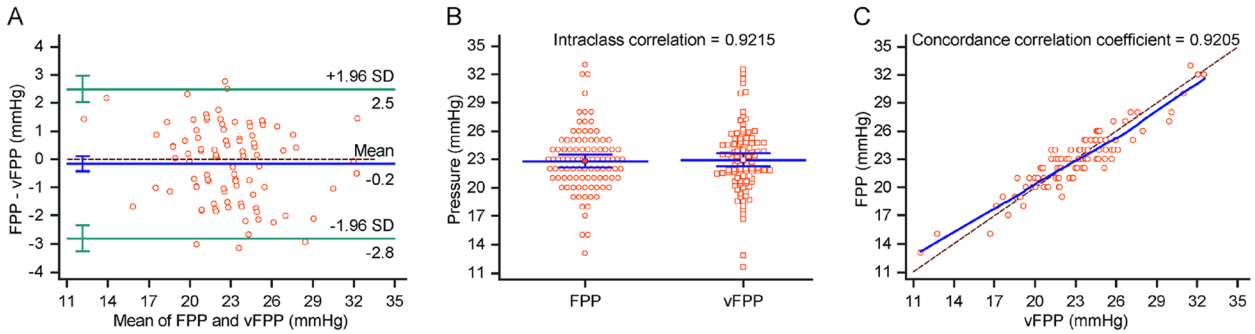

Fig. 4 The numeric correlation between vFPP and FPP. **A** Bland–Altman Limits of Agreement analysis. **B** Intraclass correlation coefficient. **C** Lin's concordance correlation coefficient. FPP, free portal pressure; vFPP, virtual free portal pressure

based on various new techniques for assessing PHT, such as color Doppler ultrasound, CT, magnetic resonance angiography, and liver transient elastography, turn out to be either inaccurate or unstable, which limits their clinical application [29–32].

We hope to establish a computational program to obtain FPP in blood vessels by combining theoretical formulas with three-dimensional simulation. Since the inner diameters of the vessels are much larger than the diameters of blood cells, and the blood flow is relatively steady and fast in these big vessels, the whole blood can be assumed to be an incompressible Newtonian fluid, and thus the blood flow can also be modeled by the Navier–Stokes equations. With the help of FLUENT software, after we import the blood vessel geometry, blood physical property, and blood vessel boundary into the software, we are able to obtain the blood flow simulation and the pressure, which is easy to apply.

In the present study, we found out that the vFPP of patients with PHT, whatever the etiology was, had a strong correlation with FPP, so it could be applied as a non-invasive method to evaluate the severity of PHT in patients. The investigators creatively introduced the method of biofluid mechanics into the field of portal pressure measurement, which was the achievement of the medico-engineering cooperation. The examinations required for calculating vFPP were clinically routine tests, which were simple and convenient for patients. Color Doppler ultrasound was used to detect the blood flow velocity and the vascular inner diameters had been commonly applied, which was different from the measurement of pressure by directly using ultrasound. In order to guarantee the stability of these results, all measurements for each patient were performed in triplicates, and the mean value was finally calculated. However, in our study, there were 118 patients included and 21 patients still excluded due to the failure or poor results of the Doppler ultrasound. The reason is many PHT patients are complicated with ascites makes it difficult to obtain good data by ultrasound measurement. In addition, there are some patients with good general conditions before admission, but during the hospitalization occurring acute bleeding, surgery for saving life is the first, and there is no more time for portal venous system ultrasound examination. The CTA, blood viscosity, and blood density examinations were also safe for the patients.

Notably, the pressure of the main portal vein and its branches can be obtained, such as the right and left branches portal vein, superior and inferior mesenteric vein, and splenic vein, as shown in Fig. 3. Thus, this is not only significant as a choice for the operation, diagnosis, and prognosis of PHT, but also helpful for other vascular system diseases such as the spleen, mesenteric, and so on. It has been verified in our previous study that the hemodynamic parameters of peripheral venous blood and portal blood are similar, so the hydrodynamic parameters of peripheral venous blood can be directly used for research in this study [38]. Furthermore, the measurement of vFPP is meaningful for the periodic reexamination of patients with PHT after surgery. Considering the complicated calculation process, we will develop software in the future, so that doctors will get the simulated FPP values only by clicking the mouse, if this portal model is proven to be credible. Therefore, it will be convenient for doctors to timely and accurately evaluate the FPP of patients with liver diseases in the future, and helpful for diagnosing and evaluating the severity of liver cirrhosis and PHT.

In this study, there were some limitations. First of all, these patients were diagnosed as PHT and underwent surgical treatment. Thus, the receiver operating characteristic (ROC) curve was not conducted in the present study. Second, the present method was only suitable for patients with PHT. Further verifications are needed to determine whether the method could

be used on patients without PHT. In addition, we are now conducting a retrospective, randomized, non-controlled, multi-center trial (trial registration number: NCT 03470389) to further verify the effectiveness of this model in predicting HVPG [39]. This would expand the application of this method, and allow it to have greater applicability. Third, after general anesthesia and abdominal incision, the intra-abdominal pressure might have changed, which might affect FPP. Fourth, there were still some difficulties in implementing Doppler ultrasound measurements. Due to the interference of air in the gastrointestinal tract, it was difficult to obtain the maximum blood flow velocity and the blood flow direction in each position. As the blood flow of the portal vein system followed the principle of conservation of mass, we could calculate some missing data. Data of the portal vein was important and necessary; of the left and right branches of the portal system, only one was necessary; of the superior mesenteric vein and the splenic vein, only one was necessary. In many cases, if the inferior mesenteric vein did not directly flow into the portal system, the data of the inferior mesenteric vein was unnecessary. Although the calculation could be carried out in the absence of some data, the results might be inaccurate. According to some reports, MRI could also obtain the velocity of blood vessels and the blood flow direction, which might serve as an alternative [40]. Fifth, our study did not conduct a subgroup analysis due to the limited sample size. We will improve the analysis in our future studies.

In conclusion, the vFPP, calculated by computational biofluid mechanics, exhibited a significant correlation with FPP in patients with PHT. The noninvasive and biofluid mechanics-based model was able to predict FPP accurately, which could be applied as a novel, non-invasive, and accurate method to evaluate portal pressure in patients undergoing surgery.

Acknowledgements
The authors thank Xiao-Yu Yang for his guidance on how to use the FLUENT software.

Authors' contributions
Lei Zheng, Guangbo Wu, and Jiayun Lin participated in the design of the research project and the writing and revision of the manuscript. Hongjie Li, Chihao Zhang, Zhifeng Zhao, Min Chen, Zhenghao Wu, Guqing Luo, Qiang Fan, and Xiaoliang Qi participated in the discussion, manuscript writing, data collection, and specific implementation of the experimental plan. Haizhong Huo, Longci Sun and Meng Luo provided funding support, multi-center joint negotiation, theme design of the project, precise design and debugging of experimental models, etc.

Funding
This study was supported by Postdoctoral Scientific Research Foundation of Shanghai Ninth People's Hospital, Shanghai Jiao Tong University School of Medicine (202401023), Clinical Research Program of 9th People's Hospital, Shanghai Jiao Tong University School of Medicine (JYLJ202124), Shanghai Municipal Commission of Health and Family Planning (20234Y0132, 20244Y0195), Shanghai Science and Technology Program (22015830900), Natural Science Foundation of Xinjiang Uygur Autonomous Region (2022D01F17), the Fundamental Research Program Funding of Ninth People's Hospital affiliated to Shanghai Jiao Tong University School of Medicine (JYZZ162), and National Natural Science Foundation of China (82100639, 82200630, 81970526).

Data availability
The research team reserves and is willing to provide all raw data involved in model analysis. If needed, please feel free to inquire via email.

Declarations

Ethics approval and consent to participate
The study conformed to the Helsinki declaration. Ethics approval and written informed consent were obtained. Furthermore, the present research was registered in the Chinese Clinical Trial Registry (Registration number: ChiCTR-DDD-17012700). The study was submitted and approved by the Ethical Committee of Shanghai Ninth People's Hospital, Shanghai Jiao Tong University School of Medicine, China (Approval No: SH9H-2021-A233-SB, SH9H-2021-TK116-1, SH9H-2019-A201-2, and SH9H-2021-T451-2).

Consent for publication
All authors have approved the manuscript and agree with its submission to Trials.

Competing interests
No benefits in any form have been or will be received from a commercial party related directly or indirectly to the subject of this manuscript and all authors have no conflicts of interest to disclose.

Author details
[1]Department of General Surgery, Shanghai Ninth People's Hospital, Shanghai Jiao Tong University School of Medicine, Shanghai 200011, People's Republic of China. [2]Department of Gastrointestinal Surgery, Shanghai Renji Hospital, Shanghai Jiao Tong University School of Medicine, Shanghai 200127, People's Republic of China.

Received: 1 March 2024 Accepted: 17 March 2025
Published online: 21 May 2025

References

1. Tsochatzis EA, Bosch J, Burroughs AK. Liver cirrhosis. Lancet. 2014;383(9930):1749–61.
2. Qi X, Berzigotti A, Cardenas A, et al. Emerging non-invasive approaches for diagnosis and monitoring of portal hypertension. Lancet Gastroenterol Hepatol. 2018;3(10):708–19.
3. Procopet B, Tantau M, Bureau C. Are there any alternative methods to hepatic venous pressure gradient in portal hypertension assessment? Journal of gastrointestinal and liver diseases : JGLD. 2013;22(1):73–8.
4. Gana JC, Serrano CA, Ling SC. Angiogenesis and portal-systemic collaterals in portal hypertension. Ann Hepatol. 2016;15(3):303–13.
5. Garcia-Tsao G, Abraldes JG, Berzigotti A, et al. Portal hypertensive bleeding in cirrhosis: Risk stratification, diagnosis, and management: 2016 practice guidance by the American Association for the study of liver diseases. Hepatology (Baltimore, MD). 2017;65(1):310–35.
6. Bosch J, Abraldes JG, Berzigotti A, et al. The clinical use of HVPG measurements in chronic liver disease. Nat Rev Gastroenterol Hepatol. 2009;6(10):573–82.
7. La Mura V, Garcia-Guix M, Berzigotti A, et al. A Prognostic Strategy Based on Stage of Cirrhosis and HVPG to Improve Risk Stratification After Variceal Bleeding. Hepatology (Baltimore, MD). 2020;72(4):1353–65.
8. de Franchis R, Dell'Era A. Invasive and noninvasive methods to diagnose portal hypertension and esophageal varices. Clin Liver Dis. 2014;18(2):293–302.
9. Garcia-Tsao G, Groszmann RJ, Fisher RL, et al. Portal pressure, presence of gastroesophageal varices and variceal bleeding. Hepatology (Baltimore, MD). 1985;5(3):419–24.

10. Zhai L, Qiu LY, Zu Y, et al. Contrast-enhanced ultrasound for quantitative assessment of portal pressure in canine liver fibrosis. World J Gastroenterol. 2015;21(15):4509–16.
11. Sherlock S. Portal circulation and portal hypertension. Gut. 1978;19(1):70–83.
12. Singal AK, Ahmad M, Soloway RD. Duplex Doppler ultrasound examination of the portal venous system: an emerging novel technique for the estimation of portal vein pressure. Dig Dis Sci. 2010;55(5):1230–40.
13. Nanashima A, Abo T, Kudo T, et al. Usefulness of examining hepatic functional volume using technetium-99m galactosyl serum albumin scintigraphy in hepatocellular carcinoma. Nucl Med Commun. 2013;34(5):478–88.
14. Palaniyappan N, Cox E, Bradley C, et al. Non-invasive assessment of portal hypertension using quantitative magnetic resonance imaging. J Hepatol. 2016;65(6):1131–9.
15. Lee JY, Kim TY, Jeong WK, et al. Clinically severe portal hypertension: role of multi-detector row CT features in diagnosis. Dig Dis Sci. 2014;59(9):2333–43.
16. Berzigotti A, Seijo S, Arena U, et al. Elastography, spleen size, and platelet count identify portal hypertension in patients with compensated cirrhosis. Gastroenterology. 2013;144(1):102-11.e1.
17. Castera L, Pinzani M, Bosch J. Non invasive evaluation of portal hypertension using transient elastography. J Hepatol. 2012;56(3):696–703.
18. Pavic T, Mikolasevic I, Kralj D, et al. Role of Endoscopic Ultrasound in Liver Disease: Where Do We Stand? Diagnostics (Basel). 2021;11(11).
19. Berzigotti A. Non-invasive evaluation of portal hypertension using ultrasound elastography. J Hepatol. 2017;67(2):399–411.
20. Zamir M, Moore JE Jr, Fujioka H, et al. Biofluid mechanics of special organs and the issue of system control Sixth International Bio-Fluid Mechanics Symposium and Workshop, March 28–30, 2008 Pasadena. California Ann Biomed Eng. 2010;38(3):1204–15.
21. Elad D, Bluestein D. Biofluid mechanics: innovations and challenges. J Biomech. 2013;46(2):207.
22. Bagnoli P, Malagutti N, Gastaldi D, et al. Computational finite element model of cardiac torsion. Int J Artif Organs. 2011;34(1):44–53.
23. Berthe A, Gartlein S, Lederer C, et al. Flow field of a novel implantable valveless counterpulsation heart assist device. Ann Biomed Eng. 2012;40(9):1982–95.
24. Debbaut C, Vierendeels J, Casteleyn C, et al. Perfusion characteristics of the human hepatic microcirculation based on three-dimensional reconstructions and computational fluid dynamic analysis. J Biomech Eng. 2012;134(1): 011003.
25. Koo BK, Erglis A, Doh JH, et al. Diagnosis of ischemia-causing coronary stenoses by noninvasive fractional flow reserve computed from coronary computed tomographic angiograms. Results from the prospective multicenter DISCOVER-FLOW (Diagnosis of Ischemia-Causing Stenoses Obtained Via Noninvasive Fractional Flow Reserve) study. J Am College Cardiol. 2011;58(19):1989–97.
26. Qi X, Zhou F, Lv H, et al. A novel noninvasive assessment of hepatic venous pressure gradient and portal pressure computed from computed tomography angiography. Arch Med Sci. 2014;10(5):1052–4.
27. Qi X, Li Z, Huang J, et al. Virtual portal pressure gradient from anatomic CT angiography. Gut. 2015;64(6):1004–5.
28. Qi X, An W, Liu F, et al. Virtual Hepatic Venous Pressure Gradient with CT Angiography (CHESS 1601): A Prospective Multicenter Study for the Noninvasive Diagnosis of Portal Hypertension. Radiology. 2019;290(2):370–7.
29. Verdonck P, Dumont K. Biofluid mechanics and the circulatory system. Technology and health care : official journal of the European Society for Engineering and Medicine. 2011;19(3):205–15.
30. Liu F, Ning Z, Liu Y, et al. Development and validation of a radiomics signature for clinically significant portal hypertension in cirrhosis (CHESS1701): a prospective multicenter study. EBioMedicine. 2018;36:151–8.
31. Liepsch D. Biofluid mechanics–an interdisciplinary research area of the future. Technology and health care : official journal of the European Society for Engineering and Medicine. 2006;14(4–5):209–14.
32. Lin JY, Zhang CH, Zheng L, et al. Assessment of a biofluid mechanics-based model for calculating portal pressure in canines. BMC Vet Res. 2020;16(1):308.
33. Groszmann RJ, Wongcharatrawee S. The hepatic venous pressure gradient: anything worth doing should be done right. Hepatology. 2004;39(2):280–2.
34. Simbrunner B, Marculescu R, Scheiner B, et al. Non-invasive detection of portal hypertension by enhanced liver fibrosis score in patients with different aetiologies of advanced chronic liver disease. Liver Int. 2020;40(7):1713–24.
35. Pons M, Augustin S, Scheiner B, et al. Noninvasive Diagnosis of Portal Hypertension in Patients With Compensated Advanced Chronic Liver Disease. Am J Gastroenterol. 2021;116(4):723–32.
36. Abraldes JG, Sarlieve P, Tandon P. Measurement of portal pressure. Clin Liver Dis. 2014;18(4):779–92.
37. Liu Y, Ning Z, Ormeci N, et al. Deep Convolutional Neural Network-Aided Detection of Portal Hypertension in Patients With Cirrhosis. Clin Gastroenterol Hepatol. 2020;18(13):2998-3007 e5.
38. Zheng L, Sun L, Zhang C, et al. Comparison of physical parameter measurements between peripheral and portal blood samples in patients with portal hypertension. Technol Health Care. 2017;25(6):1147–55.
39. Lin JY, Zhang CH, Zheng L, et al. Establishment and assessment of the hepatic venous pressure gradient using biofluid mechanics (HVPGBFM): protocol for a prospective, randomised, non-controlled, multicentre study. BMJ Open. 2019;9(12): e028518.
40. Stankovic Z. Four-dimensional flow magnetic resonance imaging in cirrhosis. World J Gastroenterol. 2016;22(1):89–102.

Publisher's Note